A lagged response to the 11 year solar cycle in observed winter Atlantic/European weather patterns

JOURNAL OF GEOPHYSICAL RESEARCH: ATMOSPHERES, VOL. 118, 13,405–13,420, doi:10.1002/2013JD020062, 2013

A lagged response to the 11 year solar cycle in observed winter Atlantic/European weather patterns

Lesley J. Gray,[1] Adam A. Scaife,[2] Daniel M. Mitchell,[1] Scott Osprey,[1] Sarah Ineson,[2] Steven Hardiman,[2] Neal Butchart,[2] Jeff Knight,[2] Rowan Sutton,[3] and Kunihiko Kodera[4]

Received 19 April 2013; revised 14 October 2013; accepted 28 October 2013; published 20 December 2013.

[1] The surface response to 11 year solar cycle variations is investigated by analyzing the long-term mean sea level pressure and sea surface temperature observations for the period 1870–2010. The analysis reveals a statistically significant 11 year solar signal over Europe, and the North Atlantic provided that the data are lagged by a few years. The delayed signal resembles the positive phase of the North Atlantic Oscillation (NAO) following a solar maximum. The corresponding sea surface temperature response is consistent with this. A similar analysis is performed on long-term climate simulations from a coupled ocean-atmosphere version of the Hadley Centre model that has an extended upper lid so that influences of solar variability via the stratosphere are well resolved. The model reproduces the positive NAO signal over the Atlantic/European sector, but the lag of the surface response is not well reproduced. Possible mechanisms for the lagged nature of the observed response are discussed.

Citation: Gray, L. J., A. A. Scaife, D. M. Mitchell, S. Osprey, S. Ineson, S. Hardiman, N. Butchart, J. Knight, R. Sutton, and K. Kodera (2013), A lagged response to the 11 year solar cycle in observed winter Atlantic/European weather patterns, *J. Geophys. Res. Atmos.*, *118*, 13,405–13,420, doi:10.1002/2013JD020062.

1. Introduction

[2] Investigations of influences of solar variability on weather and climate have a long history (see, e.g., the recent review by *Gray et al.* [2010]). Influences of relatively long term solar variations on surface climate have been demonstrated by paleoclimate data studies [e.g., *Mann et al.*, 2009], but influences of the 11 year solar cycle variation are more controversial. In recent years, as data records have become longer and more accurate, further tantalizing evidence has emerged for an influence of the 11 year solar signal although there has been much skepticism and controversy, primarily because of the difficulty of distinguishing a relatively small solar cycle influence from the internal decadal-scale variability of the atmosphere-ocean coupled system [e.g., *Pittock*, 1978, 1983, 2009; *van Oldenborgh et al.*, 2013]. The 11 year variation in the Sun's total output is small and amounts to only ~0.07% (0.17 Wm^{-2}). The direct radiative impact of the 11 year solar cycle at the Earth's surface is therefore very small, but various amplifying mechanisms have been proposed that suggest that regional responses may be much larger [*Haigh*, 1996; *Meehl et al.*, 2009].

[3] In the stratosphere, there is a well-documented 11 year solar signal in temperature associated with variations in UV absorption and ozone changes [*Gray et al.*, 2010]. These temperature changes affect the background wind distribution that influences wave propagation in winter [*Kodera and Kuroda*, 2002]. There is growing evidence of an 11 year solar response in the strength of the Northern Hemisphere (NH) polar vortex as a result of this, although it is complicated by the influence of the quasi-biennial oscillation (QBO) [*Labitzke*, 1987; *Labitzke et al.*, 2006] and natural internal variability, which is large in this region [see *Gray et al.*, 2010, and references therein].

[4] At the surface, the observational evidence is less well established. At the equator, where the Sun's radiative input is largest, there has been much recent debate about the pattern and timing of the 11 year solar signal in the observed tropical Pacific sea surface temperatures (SSTs), and whether or not 11 year solar irradiance variability at the Earth's surface can act as a trigger for El Niño–Southern Oscillation (ENSO) variability [e.g., *van Loon et al.*, 2007; *van Loon and Meehl*, 2008; *Meehl et al.*, 2008, 2009; *Roy and Haigh*, 2010; *Zhou and Tung*, 2010; *Haam and Tung*, 2012; *Roy and Haigh*, 2012].

[5] At midlatitudes, there has been similar controversy. Figure 1 shows the time series of normalized December–January–February (DJF)-averaged North Atlantic Oscillation (NAO) index [*Jones et al.*, 1997] for the period 1821–2010 with the corresponding sunspot number time series superimposed. During some periods, for example, around 1840–1860 and

Correction added on April 24 after original publication: the copyright line and license terms have been amended.

[1]NCAS-Climate, Atmospheric, Oceanic and Planetary Physics, Department of Physics, Oxford University, Oxford, UK.
[2]Met Office Hadley Centre, Exeter, UK.
[3]NCAS-Climate, Department of Meteorology, University of Reading, Reading, UK.
[4]Graduate School of Environmental Studies, Nagoya University, Nagoya, Japan.

Corresponding author: L. J. Gray, NCAS-Climate, Atmospheric, Oceanic and Planetary Physics, Department of Physics, Oxford University, Clarendon Laboratory, Parks Rd., Oxford OX1 3PU, UK. (Gray@atm.ox.ac.uk)

2169-897X/13/10.1002/2013JD020062

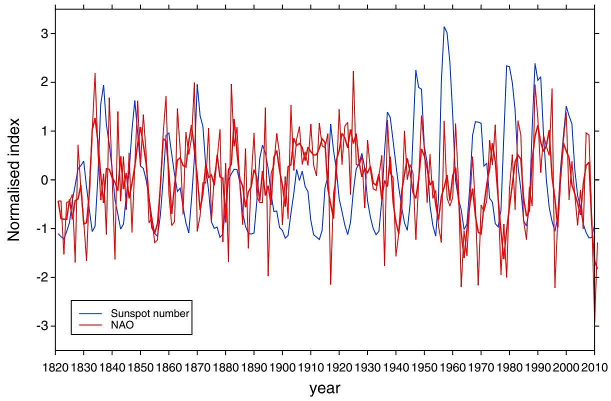

Figure 1. Time series of normalized annual-averaged sunspot number (blue) and DJF-averaged NAO index (red; thick line is running 3 year average) for 1821–2011. The NAO index is derived using the pressure difference between Gibraltar and Iceland (see text).

1980–2005, the 11 year solar cycle and NAO appear to be reasonably well correlated, but this is by no means the case throughout the whole data period, and the signals appear to be anticorrelated in the interval 1910–1930.

[6] Observational studies of the past few decades have suggested an 11 year cycle in the strength/position of the mid-latitude jet streams [*Kodera*, 2002; *Haigh*, 2003], the North Atlantic Oscillation (NAO) and Northern Hemisphere (NH) blocking frequency [*Barriopedro et al*., 2008; *Woollings et al*., 2010], but looking further back in time the signal is less convincing, giving rise to suggestions that the correlations are purely coincidental [*Rodwell*, 2003]. On the other hand, model studies that include 11 year solar variations and can be run for many years to overcome the problem of statistical significance have suggested the possibility of an 11 year solar influence over the Atlantic/European sector in wintertime [*Haigh*, 1996; *Kodera*, 2002; *Kuroda and Kodera*, 2004; *Haigh and Blackburn*, 2006; *Matthes et al*., 2004, 2006; *Ineson et al*., 2011].

[7] In a recent study of the solar signal over Europe extending back over a 250 year period, *Brugnara et al*. [2013] found a statistically significant signal over Europe but suggested that it was connected to the more meridional Eurasian pattern rather than the NAO itself. *Woollings et al*. [2010] also noted that while the circulation anomalies strongly resemble the NAO, they also extended deeper into Eurasia, especially in solar maximum periods [see also *Kodera*, 2003].

[8] There are, of course, other factors that could mask the existence of a solar signal, including simple internal unforced variability, the ENSO, sporadic volcanic eruptions, the QBO, and the response to climate forcings such as the growing levels of CO_2 in the atmosphere. Additionally, in a nonlinear system with multiple complex forcings and feedback processes, it should not be surprising if the system displays behavior that is highly complex and sporadic [*Lorenz*, 1963].

[9] Despite the difficulties of isolating and characterizing the signal that has given rise to the various controversies outlined above, it is nevertheless important to continue to examine the observational evidence using whatever practical analysis tools are available and to investigate possible amplification mechanisms so that the presence or otherwise of an 11 year solar cycle influence may be established. The NAO is the major mode of variability in the North Atlantic/European sector and serves as a good indicator of seasonal European weather. Hence, if an 11 year solar-related signal is confirmed, it offers a potential source of information that could improve seasonal to decadal weather forecasts, particularly on regional scales.

[10] In this paper, we address these issues by reexamining observations of mean sea level pressure (mslp) and sea surface temperatures (SSTs) back to the midnineteenth century with a particular focus on the North Atlantic/European sector. We employ a multiple linear regression analysis technique in which the time and spatial variations of the observations are represented using an optimum least squares fit to a combination of relevant "forcing" indices that represent the major possible influences (volcanic, ENSO, solar, and anthropogenic). Although there are limitations to this technique, such as the assumption of linearity and the possibility of degeneracy between the indices employed, the technique has been usefully employed to investigate the solar signal in various atmospheric and surface data sets [*Haigh*, 2003; *Crooks and Gray*, 2005; *Lean and Rind*, 2008, 2009; *Frame and Gray*, 2010; *Roy and Haigh*, 2010].

[11] The prime pitfall of degeneracy between the forcing indices employed in multiple linear regression analyses arises when the forcing indices are insufficiently distinct from one another so the signals may be aliased to give a false signal [e.g., *Ingram*, 2006]. This is a particular problem when trying to extract the signal associated with the long-term underlying trend in solar output which can be difficult to distinguish from trends due to increased greenhouse gas levels. For this reason, we concentrate here only on the 11 year solar variation. Similarly, there is a possibility of aliasing between the 11 year solar and volcanic signals. This is a concern when analyzing data for the recent past [*Frame and Gray*, 2010] since the El Chichon and Pinatubo eruptions occurred approximately 11 years apart and coincided with solar maxima. However, over the much longer period examined in this study (1870–2010), the time evolution of the two indices is sufficiently distinct that this is no longer an issue. There is also the possibility that the 11 year solar and the ENSO signals could be aliased. Sensitivity tests in which one or other of the solar and ENSO indices was excluded, confirming that the pattern and magnitude of the two responses from our study are not unduly influenced by the presence or absence of the other and increasing our confidence that the solar signal is not a spurious artifact of the analysis. Finally, although the influence of the QBO and its possible (nonlinear) interaction with the solar cycle is important to represent when examining the stratospheric response, it cannot be included in the analysis of surface observations that extend back to 1870 because there are no available QBO indices that extend far enough back in time.

[12] Our study extends previous analyses by looking additionally at *lagged* regressions so that we can characterize the temporal as well as spatial patterns of the 11 year solar response. While the results of the analysis are presented over the entire globe for comparison with previous studies [notably *Roy and Haigh*, 2010; *Zhou and Tung*, 2010], we concentrate our analysis primarily on the wintertime North Atlantic/European sector. The study is similar to that of

Hood et al. [2013] although they concentrate on the solar response over the Pacific region and examine lead/lag times of only ±2 years. Our analysis reveals an emerging signal that resembles a positive NAO response following solar maxima with a lag of approximately 3–4 years.

[13] In addition, we compare these observational results with simulations using the Hadley Centre coupled ocean-atmosphere climate model (HadGEM2) using the same regression technique. Although the model captures reasonably well the pattern of solar response, it fails to capture the lagged nature of the response.

[14] The layout of the paper is as follows: In section 2, we describe the data sets, the model, and the methodology employed. The observational results are presented in section 3. Climate model simulations are described in section 4 and compared with the observational results. Section 5 provides a summary of the main findings and a discussion of possible mechanisms.

2. Methods and Data Sets

2.1. Observational Data Sets

[15] Mean sea level pressure data (mslp; hPa) for 1850–2004 were analyzed from the UK Hadley Centre Sea Level Pressure (HadSLP2) data set [*Allan and Ansell*, 2006] and updated to 2010 by the HadSLP2r data set. Sea surface temperature data (SST; K) for 1870–2010 were from the Hadley Centre Sea Ice and Sea Surface Temperature (HadISST) data set [*Rayner et al*., 2003]. All three data sets are available from the Hadley Centre website (www.metoffice.gov.uk/hadobs/) and are based on pure observations rather than reanalysis to allow a clear distinction to be made from models. The analysis was also repeated using the extended reconstructed SST (ERSST) data set (http://www.cdc.noaa.gov/cdc/data.noaa) with similar results, so only the HadISST results are shown here. Since the mslp and SST data sets are not the same in length and the results from the mslp analysis were found to be unaltered by the inclusion or otherwise of the first 20 years of the data set, we only show results for 1870–2010.

[16] For the estimation of the observed 11 year solar variation in equatorial stratopause temperatures (Figure 6), zonally averaged temperature data from the European Centre for Medium-Range Weather Forecasts (ECMWF) Re-Analysis data set (ERA-40), updated by the operational data to cover the period 1979–2008, were employed (see *Frame and Gray* [2010] for details).

[17] The NAO values in Figure 1 are the monthly averages available from 1821 on the University of East Anglia Climate Research Unit website (http://www.cru.uea.ac.uk/~timo/datapages/naoi.htm). They have been derived by taking the mean sea level pressure differences between Gibraltar and Iceland [*Jones et al*., 1997].

2.2. The Model

[18] The climate simulations described in section 4 were generated by the UK Met Office Hadley Centre coupled ocean-atmosphere Global Environment Model (HadGEM). The version employed was the HadGEM2-CCS version, as described by *Martin et al*. [2011]. The atmospheric component has horizontal resolution of 1.875° longitude × 1.25° latitude with 60 vertical levels extending from the surface to approximately 84 km. A detailed examination of the stratospheric climatology and variability in this model has been reported by *Hardiman et al*. [2010] and *Osprey et al*. [2010]. The model includes a momentum-conserving nonorographic gravity wave drag parameterization [*Warner and McIntyre*, 1999; *Scaife et al*., 2002] and has a self-generated quasi-biennial oscillation (QBO) as a result of this. The oceanic component Hadley Centre Ocean Carbon Cycle has a horizontal resolution of 1° × 1° increasing in the tropics to 0.3° with 40 vertical levels and a lower boundary at 5.3 km. The model includes a coupled carbon cycle, but there is no explicit interactive chemistry apart from methane oxidation.

[19] The climate simulations cover the period 1860–2100 and were prepared as input to the Coupled Model Intercomparison Project (CMIP5). They include a representation of all known forcings as described in detail by *Jones et al*. [2011] with realistic increases of greenhouse gases, imposed variations of volcanic aerosol optical depths using the updated *Sato et al*. [1993] data set and a representation of solar variability. During the historical period, the prescribed CO_2, methane, and other greenhouse gases are specified according to the CMIP5 recommendations, and in the future, they followed the Representative Concentration Pathway RCP8.5. The imposed historical stratospheric ozone amounts included a realistic seasonal cycle and ozone hole development since the 1980s and used the average estimation from chemistry-climate model projections for the future [*Cionni et al*., 2011].

[20] Solar irradiance variations were imposed by partitioning the total solar irradiance (TSI) variations across the six shortwave spectral bands in the model (0.2–10 μm) with the associated Rayleigh scattering and ozone absorption variations [*Stott et al*., 2006]. The TSI data for the historical period were those recommended by CMIP5 [*Wang et al*., 2005; *Lean*, 2009] and include both an 11 year variation and a longer-term underlying variation. After 2005, a repeating cycle was employed with no underlying long-term variation. The repeated cycle had a period of 11 years whose mean and maximum-minimum values corresponding to solar cycle 23. An 11 year solar cycle in ozone amounts was also imposed, based on the observational analysis of *Randel and Wu* [1999], as described by *Jones et al*. [2011, section 4.2].

[21] The solar signal in three-ensemble simulations has been analyzed. The first member extends from 1860 through to 2100. The two additional members extend from 1960 to 2100 and were initialized from the first simulation by using the atmospheric and oceanic model states from different dates in November 1959 [*Hardiman et al*., 2012]. As a result, 520 years of model simulations were available for analysis, approximately forty-seven 11 year solar cycles.

2.3. The Regression Analysis

[22] The multilinear regression analysis employed an identical approach to earlier work [*Haigh*, 2003; *Crooks and Gray*, 2005; *Frame and Gray*, 2010; *Roy and Haigh*, 2010]. For the surface observational analysis, four independent "forcing" indices were employed to represent the major sources of variability in the analyses of the observational data sets: ENSO, volcanic eruptions, the 11 year solar cycle, and the long-term trend. The QBO was not included in the surface observational analysis because there are no estimates of the QBO that extend back to 1870. However, analysis of more recent,

shorter periods in which the QBO was included showed that the QBO response at the surface was relatively small.

[23] As in *Roy and Haigh* [2010], we employ monthly sunspot numbers to represent the 11 year solar variability in the observational analysis, thus avoiding complications that arise from using total solar irradiance (TSI) data, which has an underlying long-term variation and includes assumptions about solar behavior and the relationship between solar irradiance and sunspot numbers. To represent ENSO variability, we use monthly averaged sea surface temperatures averaged over the Niño 3.4 region from the HadISST data set. The major volcanic eruptions are represented by the updated time series of monthly mean aerosol optical depth [*Sato et al*., 1993]. Finally, a linear trend is included to represent anthropogenic warming over the period. A number of sensitivity tests were performed and showed that the results were not sensitive to the exact nature of this trend term—more realistic representations, e.g., following greenhouse gas emission or concentration pathways or including a modified trend term to include tropospheric aerosol trends had little effect on the overall results.

[24] For the stratospheric temperature regression analysis (used in Figure 6), two additional indices were included to represent QBO variability. Reliable stratospheric temperature observations are only available since 1979 so the analysis of the solar response in the stratosphere was carried out only for the period since 1979 (using ERA data; see section 2.1). The two QBO indices were obtained by computing the first two empirical orthogonal functions (EOFs) of the equatorial lower stratospheric zonal wind field from the ERA data (for details, see *Crooks and Gray* [2005]). The inclusion of these two additional indices is important when characterizing the signal in the stratosphere, but sensitivity tests showed that their presence made little or no difference to the solar signal at the surface.

[25] The regression analysis of the model simulations was performed using the same regression technique and all six indices. For the solar index, however, the TSI time series of *Lean* [2009] was used instead of sunspot number, for consistency with the fact that these TSI values were used to impose the solar variations in the climate simulations. In order to examine only the 11 year component, an 11 year running mean of the TSI values was computed and subtracted from the data so that the underlying long-term solar variation was removed. The results were not sensitive to the exact length of this smoothing average provided it was sufficiently long to adequately smooth out the 11 year cycle. The extended *Sato et al*. [1993] volcanic aerosol index was employed for the volcanic eruption index. The ENSO index was derived by averaging the modeled SSTs over the Niño 3.4 region. The two QBO indices were derived by computing the first two EOFs of the modeled lower equatorial stratospheric zonal winds.

[26] An autoregressive AR(1) noise model was employed in all of the regression analyses so that the noise coefficients were calculated simultaneously with the other components of variability and were consistent with a red noise model of order one. Sensitivity tests with different orders up to AR(3) did not show significant differences. A two-tailed Student's *t* test was used to determine the 95% and 99% probabilities that the regression coefficients are significantly different from noise. The analysis concentrates on the NH winter period, so the results are shown for DJF averages unless otherwise stated. Note that the regression coefficients associated with the 11 year solar cycle from Figure 4 onward have been rescaled by the standard deviation and multiplied by the maximum peak-to-trough sunspot number in the appropriate data interval to obtain an estimate of the maximum likely response to variations in the Sun's output.

3. Observational Results

[27] Figures 2 and 3 show the global regression coefficient distributions of observed SST and mslp anomalies, respectively, for December–January–February (DJF) averages over the period 1870–2010 associated with each of the four regression indices (11 year solar cycle, volcanic, anthropogenic, and ENSO). No lags have been applied to any of the regression indices. The patterns of the responses are consistent with previous studies. For example, the ENSO SST response (Figure 2) displays the well-known warm tongue extending across the equatorial Pacific together with the corresponding mslp anomalies (Figure 3) that show the typical ENSO modulation of the Walker circulation. The volcanic signal shows generalized cooling over much of the globe in the SST response and a weak but statistically significant NAO-like response in mslp, as noted by several studies [e.g., *Driscoll et al*., 2012, and references therein]. The linear trend term shows generalized warming over most of the globe and a dipole in the mslp response over the Southern Ocean, consistent with patterns of observed changes associated with anthropogenic warming and ozone depletion [*Intergovernmental Panel on Climate Change*, 2007].

[28] *Zhou and Tung* [2010] carried out an extensive study of the solar signal in SST observations using a multiple composite mean difference approach so the distributions of the volcanic, ENSO, and anthropogenic regression coefficients in Figure 2 can be usefully compared with their results [*Zhou and Tung*, 2010, Figure 6]. As expected, the ENSO pattern agrees very well, and also, the volcanic signals have similar cooling distributions in equatorial/subtropical latitudes and a region of generalized warming near 60°S. The anthropogenic terms have a similar region of maximum warming around the southern tip of South Africa and along the NH western ocean boundaries, but the warm Pacific equatorial tongue in the Zhou and Tung results is missing from Figure 2.

[29] The 11 year solar SST response in Figure 2 is relatively weak compared with the ENSO and trend terms, but note that the significance values (dots) are plotted at the 99% level, for consistency with the other terms (larger regions are significant at the 95% level). In the east equatorial Pacific, there is a region of statistically significant weak cooling similar to that discussed by *van Loon et al*. [2007] [see also *van Loon and Meehl*, 2008; *Meehl et al*., 2008, 2009; *Meehl and Arblaster*, 2009], but it does not show a close resemblance to the ENSO distribution since the pattern shows no particular symmetry about the equator nor does it extend as far westward as the ENSO signal. In addition, the signal along the west coast of North America is of the opposite sign. In the Southern Hemisphere, there is a band of weak warm anomalies at around 50–60°S (significant at the 95% level; see Figure 5) in good agreement with the results of *Zhou and Tung* [2010] and *Hood et al*. [2013]. Although

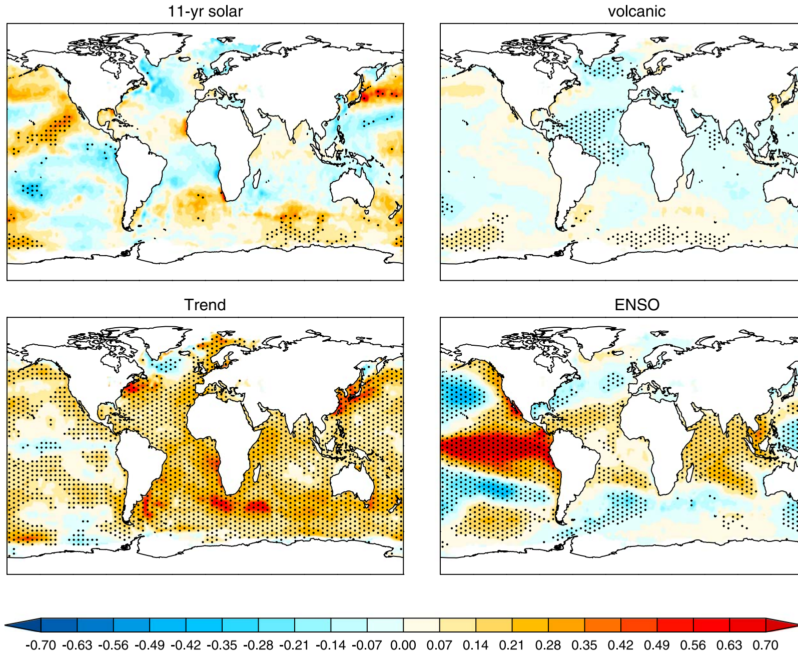

Figure 2. Regression coefficients at zero lag from the analysis of the HadISST sea surface temperature observational data set for DJF averages over the 1870–2010 period for each of the four indices employed in the regression analysis: 11 year solar cycle, volcanic, trend, and ENSO. Units are K per standard deviation for the linear trend, volcanic, and ENSO terms and K per 100 sunspot number for the 11 year solar cycle terms. Black dots denote 99% statistical significance using a two-sided Student's *t* test.

there is some evidence of a similar anomaly in the results of *Roy and Haigh* [2010] who analyzed the ERSST data set [*Roy and Haigh*, 2010, Figure 2a], it is less clear in their study. In addition, there is a statistically significant signal in Figure 2 in the northwest Pacific SSTs with a SW-NE-oriented banded structure. This response also features prominently in the analysis of *Hood et al.* [2013, Figure 4]. *Zhou and Tung* [2010] also have this tripolar SW-NE banded structure, but it is less

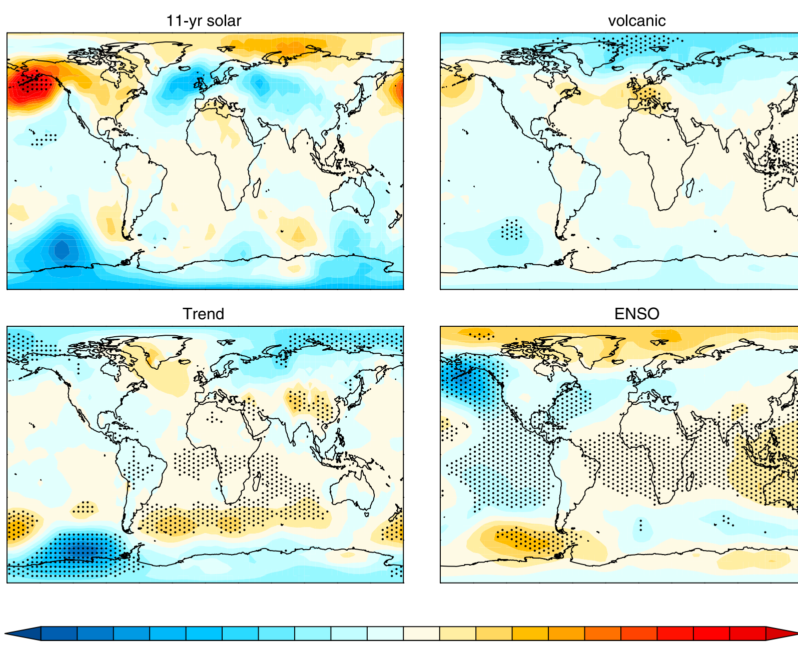

Figure 3. Regression coefficients at zero lag from the analysis of the HadSLP mean sea level pressure observational data set for DJF averages over the 1870–2010 period for each of the four indices employed in the regression analysis: 11 year solar cycle, volcanic, trend, and ENSO. Units are hPa per standard deviation for the linear trend, volcanic, and ENSO terms and K per 100 sunspot number for the 11 year solar cycle terms. Black dots denote 99% statistical significance using a two-sided Student's *t* test.

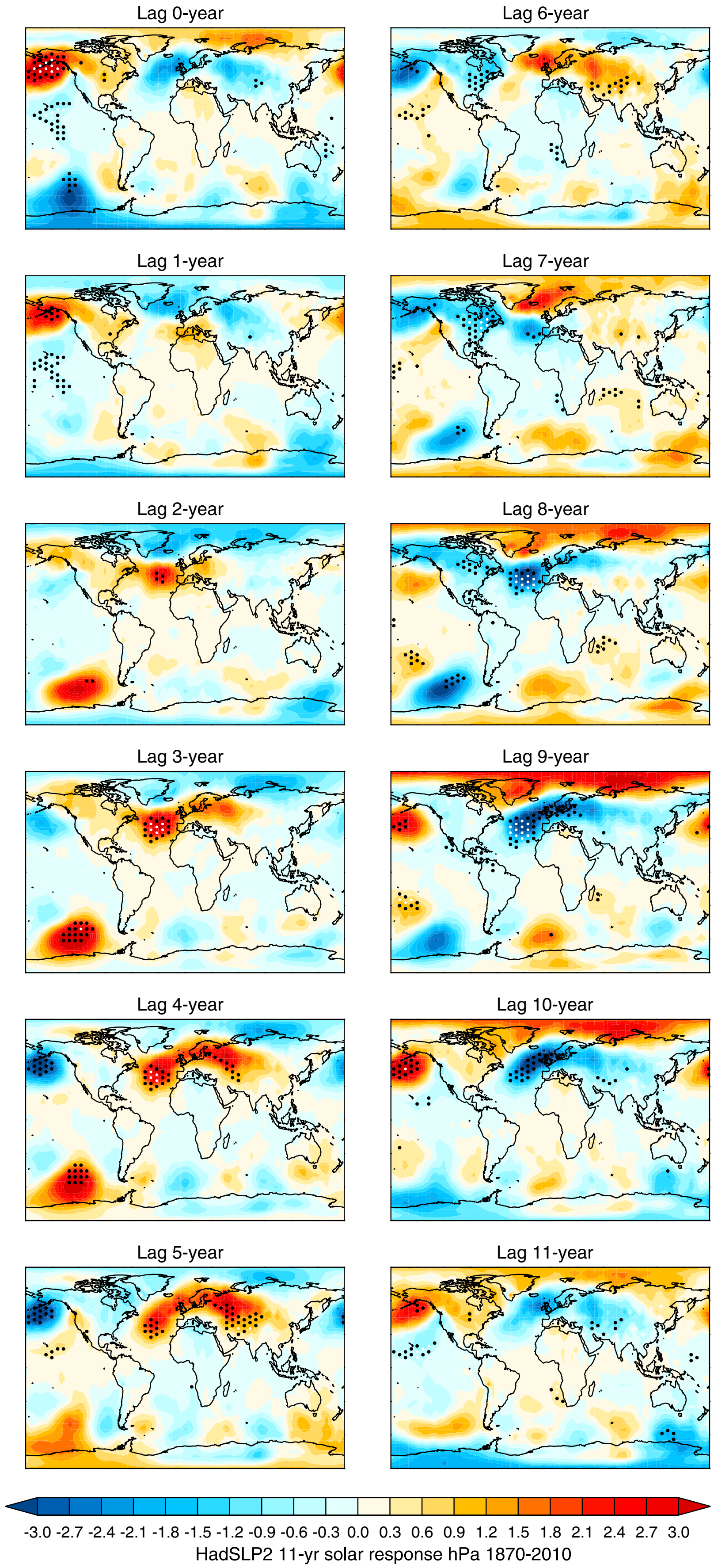
Lag 0-year
Lag 6-year
Lag 1-year
Lag 7-year
Lag 2-year
Lag 8-year
Lag 3-year
Lag 9-year
Lag 4-year
Lag 10-year
Lag 5-year
Lag 11-year
-3.0 -2.7 -2.4 -2.1 -1.8 -1.5 -1.2 -0.9 -0.6 -0.3 0.0 0.3 0.6 0.9 1.2 1.5 1.8 2.1 2.4 2.7 3.0
HadSLP2 11-yr solar response hPa 1870-2010

Figure 4

distinct. Although not the primary focus of this study, we note that this feature is similar in its structure to the horseshoe-shaped anomaly associated with the Pacific Decadal Oscillation [see, for example, *Schneider and Cornuelle*, 2005; *Deser et al*., 2010].

[30] The 11 year solar response in mslp (Figure 3) shows a statistically significant response only in the North Pacific in the region of the Aleutian Low with a region of opposite sign just south of it, so that the Aleutian Low is weaker and the Hawaiian High is slightly farther north during periods of solar maximum. This is in good agreement with the results of *Christoforou and Hameed* [1997], *van Loon et al*. [2007], *Roy and Haigh* [2010], and *Hood et al*. [2013]. We note that *Zhou and Tung* [2010] did not examine mslp fields.

[31] In the North Atlantic sector, the mslp analysis (Figure 3) shows no sign of any statistically significant mslp response to the 11 year solar signal. There is a region of negative anomaly centered to the north of the UK, similar to that seen in the composite analysis of *Brugnara et al*. [2013, Figure 3], but it is not statistically significant.

[32] A different picture emerges, however, when the *lagged* 11 year solar response in mslp is calculated. The lagged response was calculated simply by shifting the solar index a month at a time so that the surface data lag the solar index. All other indices were kept at zero lag. Figure 4 shows the 11 year solar cycle regression coefficients at yearly intervals for lags of up to 11 years. Note that the coefficients have been rescaled by the standard deviation and multiplied by the maximum peak-to-trough sunspot to give an estimate of solar maximum minus solar minimum differences.

[33] In this case, a coherent positive anomaly emerges over the Atlantic, centered over the region of the Azores (2 year lag), which then strengthens (3 year lag) and extends across into Europe (3–4 year lags). The positive signal over the Azores is statistically significant at the 95% level at all lags between 3 and 5 years, and its maximum amplitude reaches a peak of ~3 hPa at 3–4 years lags with 99% significance.

[34] The standard deviation of the full wintertime sea level pressure data (which includes all sources of variability) is ~3–4 hPa at 45°N over the North Atlantic so the 3 hPa solar signal represents a substantial shift (although note that this is a maximum estimate for the solar response and its average response is likely to be closer to half this). A corresponding anomaly of opposite sign is evident over Iceland, but the standard deviation in this region is larger so the statistical significance is not as high. The pattern of the 11 year solar response resembles the NAO, with a positive NAO phase lagging the solar maximum by ~3 years. The signal reverses in sign as the lag increases, consistent with the oscillatory nature of the solar cycle, and is statistically significant at the 95% level at 7–10 year lags and at the 99% level at 8–9 year lags. We note that although the spatial pattern of the response resembles the NAO, our analysis does not conclusively detect a solar response in the NAO index itself, because the response over Iceland is weak and statistically insignificant.

[35] The results shown in Figure 4 are generally consistent with those of *Brugnara et al*. [2013]. They examined the 11 year solar signal over Europe and the Atlantic using a different mean sea level pressure data set that extends back to 1749 [*Luterbacher et al*., 2002] and covers only the Atlantic/European region (30–70°N latitude and −30 to +40° longitude). They examined the late winter response (January–February–March as opposed to DJF) at zero lag only. At solar maximum, they found a strengthening of the Icelandic Low and a positive anomaly over northwest Africa, consistent with a positive NAO-like response, but the response over northwest Africa was not statistically significant. Their response is therefore consistent with our analysis at zero lag (Figure 4, top left), but the added years in their analysis enabled the Icelandic response to be confirmed as statistically significant. An extension of their study to include the lagged response so that the time evolution of the response over the region of the Azores can be examined would be extremely interesting. The pattern of evolution in Figure 4 is also consistent with the analysis of *Hood et al*. [2013], who noted that the mslp response evolves from a negative Arctic Oscillation (AO) response several years prior to solar maxima to a positive AO-like response following solar maxima, although their investigation only extended to lead/lag times of ±2 years.

[36] The lagged SST analysis (Figure 5) shows a spatial pattern consistent with the NAO-like sea level pressure pattern [*Visbeck et al*., 2001], and the time evolution corresponds well. A cold anomaly develops in the Labrador Sea (southwest of Greenland) at 0–1 year lags, and this deepens and extends eastward into the Atlantic (2–3 year lags) with 99% statistical significance. At lags of ~3 years, a tripolar pattern of SST anomalies is present in the Atlantic which is the typical SST response to a positive NAO [*Bjerknes*, 1964] and is also associated with anomalously warm observed temperatures over northern Europe. We note that the methods of SST data collection are independent of the mslp data collection, and hence, the 11 year signal in the SST analysis provides a good validation of the 11 year signal seen in the mslp analysis.

[37] The lagged distributions in Figures 4 and 5 show regional anomalies that wax and wane at different times during the 11 year cycle. In order to encapsulate the time evolution of these anomalies, Figure 6 shows the scaled solar regression coefficients averaged over selected regions of the globe as a function of various lag and lead times (in years). A maximum positive value at zero lag signifies a signal whose maximum positive anomaly coincides with solar max. The evolution of the Azores mslp anomaly is representative of the evolution of the positive NAO-like response at lags of 3–4 years after solar maximum. The maximum mslp anomaly in the Aleutian Low region, on the other hand, peaks at around lag zero, which explains why it has been easily identified in earlier studies that examined only the zero lag response. The East Pacific SST anomaly is also shown for

Figure 4. The 11 year solar cycle signal in DJF HadSLP mean sea level pressure data set (mslp; hPa) from the regression analysis for 1870–2010 with the mslp data lagging the sunspot index by different numbers of years. Regression coefficients have been rescaled by the standard deviation and multiplied by the maximum peak-to-trough sunspot number to give an estimate of solar maximum minus minimum differences. Black (white) dots denote 95% (99%) statistical significance using a two-sided Student *t* test.

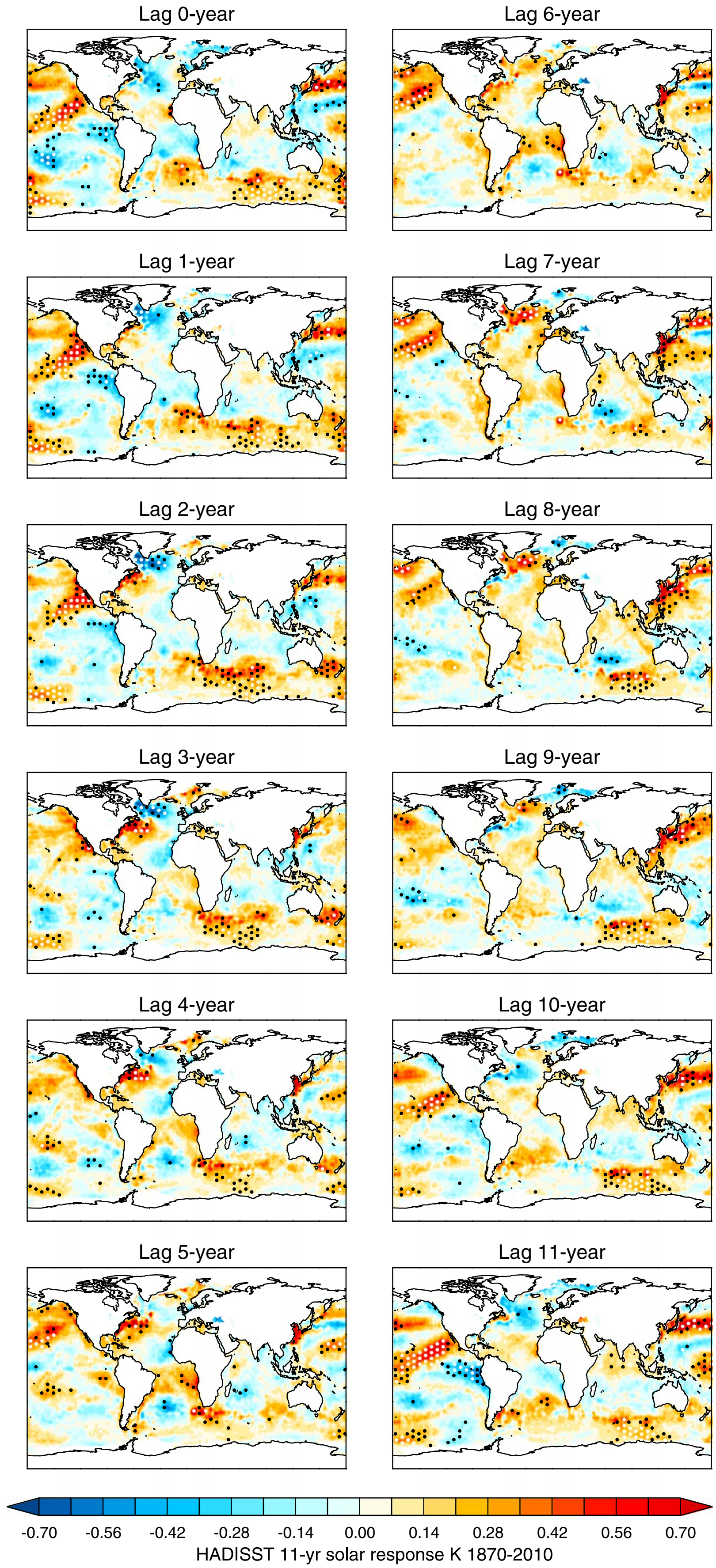

Figure 5. As Figure 4 but from the regression analysis of the HadISST sea surface temperature (K) data set.

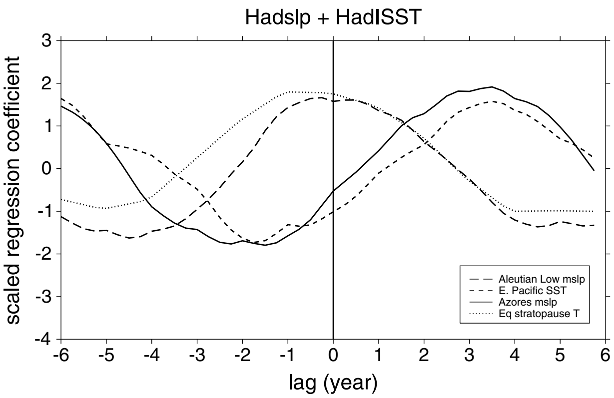

Figure 6. Regression coefficients of DJF 11 year solar cycle signal from the observational analyses at different lags and lead times for selected regions of the atmosphere and oceans mslp solar regression coefficients averaged over the Aleutian Low region (hPa; long dash) and over the Azores region (hPa; short dash) from the HadSLP analysis, SST solar coefficients averaged over the East Pacific (K; dash dot) from the HadISST analysis, and ERA analyses equatorial stratopause temperature regression coefficients (K; dots) from the ERA reanalysis. Regression coefficients have been rescaled by the standard deviation and multiplied by the maximum peak-to-trough sunspot number to give an estimate of solar maximum minus minimum differences.

comparison with studies that have concentrated on this region. Our analysis suggests a negative SST response approximately 2 years before the peak of the 11 year solar cycle and a positive response approximately 3–4 years after solar maximum.

[38] In addition, we include in Figure 6 the solar response in the region of the equatorial stratopause derived from a lagged regression analysis of zonally averaged stratospheric temperatures using ECMWF Re-Analysis data (see section 2 for details). One candidate mechanism for a surface solar cycle response at high latitudes is via anomalous heating of the equatorial upper stratosphere that alters the winter stratospheric circulation (the so-called top-down mechanism) [*Gray et al*., 2010; *Haigh*, 1996; *Kodera*, 1995; *Kodera and Kuroda*, 2002]. Increased irradiance at solar maximum generally results in warmer equatorial temperatures and a stronger, less disturbed stratospheric polar vortex although the relationship is complicated by the QBO [*Labitzke*, 1987; *Labitzke et al*., 2006]. The influence of an anomaly in the strength of the polar vortex can extend down to the surface, giving a positive NAO anomaly at the surface [*Baldwin and Dunkerton*, 2001; *Matthes et al*., 2006; *Ineson et al*., 2011; *Mitchell et al*., 2013]. Radiative timescales in the upper stratosphere are relatively short, and Figure 6 confirms that equatorial stratopause temperatures respond rapidly to the irradiance variations (although it is not clear why the maximum temperature anomalies occur slightly before the solar maximum rather than coincident with it). If the mslp response in the region of the Azores is due primarily to atmospheric forcing via the upper stratosphere, then Figure 6 suggests an unexpected lag of 3–4 years between the stratospheric response and the timing of the peak response at the surface. This is discussed further in section 5.

[39] Interestingly, the timing of the observed Aleutian mslp solar signal in Figure 6 closely follows the evolution of the stratospheric signal, with a small delay. This is consistent with it being at least partially forced via a "top-down" mechanism from the stratosphere. There may also be an additional influence from the Pacific SST solar anomaly since the Pacific SSTs are known to influence the Aleutian region through the generation of an anomalous planetary wave train in the troposphere. However, closer examination shows that the Aleutian Low solar signal increases as the East Pacific solar signal decreases, with an approximately 1–2 year lag between the peak Pacific SST solar response and the peak Aleutian Low solar response. It is not obvious why the Aleutian region would take 1–2 years to respond to a Pacific SST solar anomaly.

4. Climate Model Simulations

[40] The 11 year solar signal response has also been analyzed in climate model simulations using the HadGEM2 ocean-atmosphere model with a version that has its upper boundary at approximately 85 km. This means that the mechanism for impact of solar variability on the stratosphere via changes in UV irradiance and ozone distributions has been included (the "top-down" mechanism) in addition to the impact of variations in the visible region of the solar irradiance spectrum that influence the surface directly (the "bottom-up" mechanism). The model also includes a self-generated QBO which compares well with the observed QBO [*Osprey et al*., 2010].

[41] The HadGEM2 simulations were prepared as input to the recent Coupled Model Intercomparison Project (CMIP5). They include representation of all known forcings, including greenhouse gases, ozone, volcanic eruptions, solar cycle, and aerosol prescribed from observations for the historical period and estimated in the future following the Representative Concentration Pathway RCP8.5 (see section 2 for more details). An ensemble of three simulations were analyzed. One extended for the full period 1860–2100 and the other two for the shorter 1960–2100 period, providing a total of 520 years with approximately forty-seven 11 year solar cycles. As expected, there was some interensemble variability in the analyzed results, but all ensembles showed the same broad behavior so only results that employed all three ensembles are presented. Similarly, although we found subperiods within the model data when the solar signal was different from that of the full 520 year period (in either amplitude and/or timing), none of the subperiod results were statistically significant, so they are not presented here. Further investigation of the sporadic nature of the modeled solar cycle response would require extending the number and/or length of the model simulations.

[42] We note here that these simulations differ from those analyzed by *Ineson et al*. [2011]. In that study, a 20-member ensemble of short-duration sensitivity simulations were carried out in which a relatively large step change in UV solar irradiance (alone) was imposed. The step change was greater than the standard *Lean* [2009] values in order to test the response to the larger variation indicated by measurements from the Spectral Irradiance Monitor instrument, and no ozone variations were imposed. In contrast, the simulations analyzed here are long-duration climate simulations that

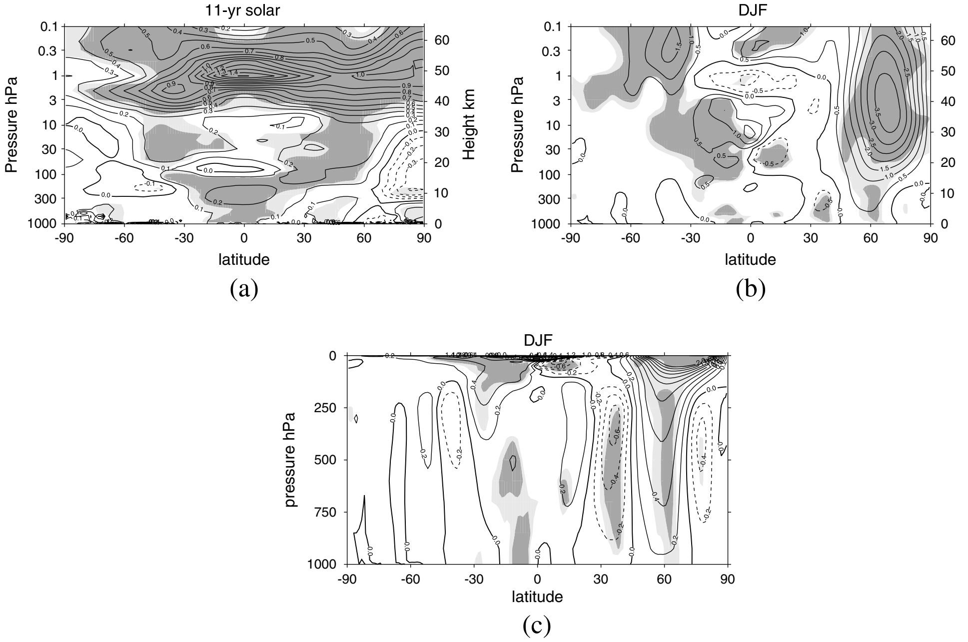

Figure 7. Modeled 11 year solar signal (solar maximum minus solar minimum) in (a) annual mean zonally averaged temperature (K), (b) DJF zonally averaged zonal winds, and (c) as Figure 7b but using a pressure scale to highlight the tropospheric structure. Two shades of grey denote 95% and 99% statistical significance using a Student's *t* test.

employ the *Lean* [2009] irradiance variations at all wavelengths (following CMIP recommendations) and also include 11 year variations in the imposed ozone distributions (see section 2). For a more detailed discussion of the effects of including different solar variability data sets on the modeled solar cycle response, see *Ermolli et al*. [2013].

[43] Figure 7a shows the modeled height—latitude cross section of the annual-averaged 11 year solar response in zonally averaged temperature. The annual average is shown for ease of comparison with observational analyses such as *Frame and Gray* [2010]. The primary response at the equatorial stratopause shows a 1.5 K increase in temperature at solar maximum compared with solar minimum, in good agreement with the observational analyses. At polar latitudes and at the equator near 10 hPa (where the QBO maximizes), statistical significance is not achieved even with 520 years of data, because of high background variability. Secondary weak maxima are present in the subtropical lower stratosphere centered around 30 hPa 30–40°N and 30 hPa 40°S, in reasonably good agreement with observations, although they are slightly weaker than those observed. *Gray et al*. [2009] examined the temperature responses associated with 11 year variations in UV irradiances and with the 11 year variations in ozone abundances. They found that both the irradiance and the ozone influences contribute to the primary temperature response at the equatorial stratopause, but the secondary temperature response in the lower stratosphere was dominated by the ozone variations, because the UV irradiance does not penetrate down to those levels. This suggests that the underestimation of the modeled temperature response at these lower stratospheric levels is most likely associated with the imposed 11 year ozone variations, which may have been underestimated. The lower equatorial stratosphere is also the region affected by volcanic, QBO, and ENSO influences, so an inadequate representation of these factors and their nonlinear interactions could also impact on the extracted solar signal in this region.

[44] Interestingly, the model also shows a significant positive temperature response in the equatorial troposphere, with a maximum in the upper troposphere. A similar upper tropospheric equatorial warming at solar max is present in the observational analysis of the NCEP data set by *Zhou and Tung* [2013] who used a composite mean difference approach, but it is not present in the regression analysis of the ECMWF data set by *Frame and Gray* [2010]. *Zhou and Tung* [2013] interpret this feature as evidence for the predominance of the "bottom-up" mechanism. Resolution of this difference between the observational analyses of *Zhou and Tung* [2013] and *Frame and Gray* [2010] is therefore required but is outside the scope of the current study.

[45] The modeled DJF-averaged solar response in zonally averaged zonal wind is shown in Figures 7b and 7c for the stratosphere and troposphere, respectively. A NH polar vortex that is stronger in solar maximum years is evident (Figure 7b), and this positive wind anomaly extends down into the troposphere (Figure 7c). The banded structure of the anomalies in the troposphere agrees well with the observed response [*Haigh and Blackburn*, 2006] and signifies a poleward shift of the midlatitude jet and a broadening of the Hadley circulation in solar maximum years. However, the maximum magnitude of the response (~0.6 ms^{-1}) is smaller than the NCEP analysis of *Haigh and Blackburn* [2006] who found a maximum response of ~2 ms^{-1}.

[46] The modeled surface response to the 11 year solar cycle is indicated by the mslp and surface (1.5 m) air temperature responses in Figures 8 and 9. The mslp response (Figure 8) can be compared with the observations in Figure 4 and shows a broad pattern of increased pressure over

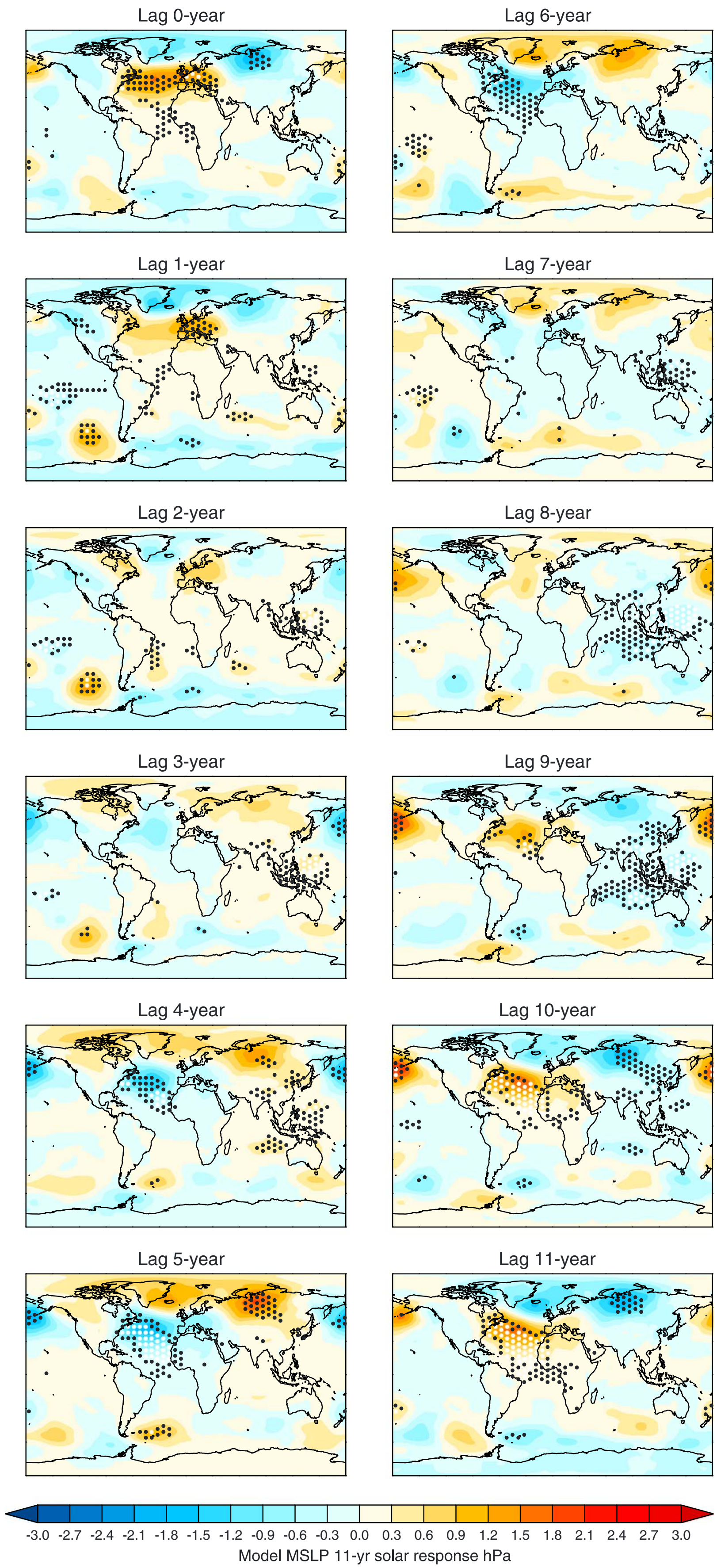

Figure 8. As Figure 4 but from the climate model simulations.

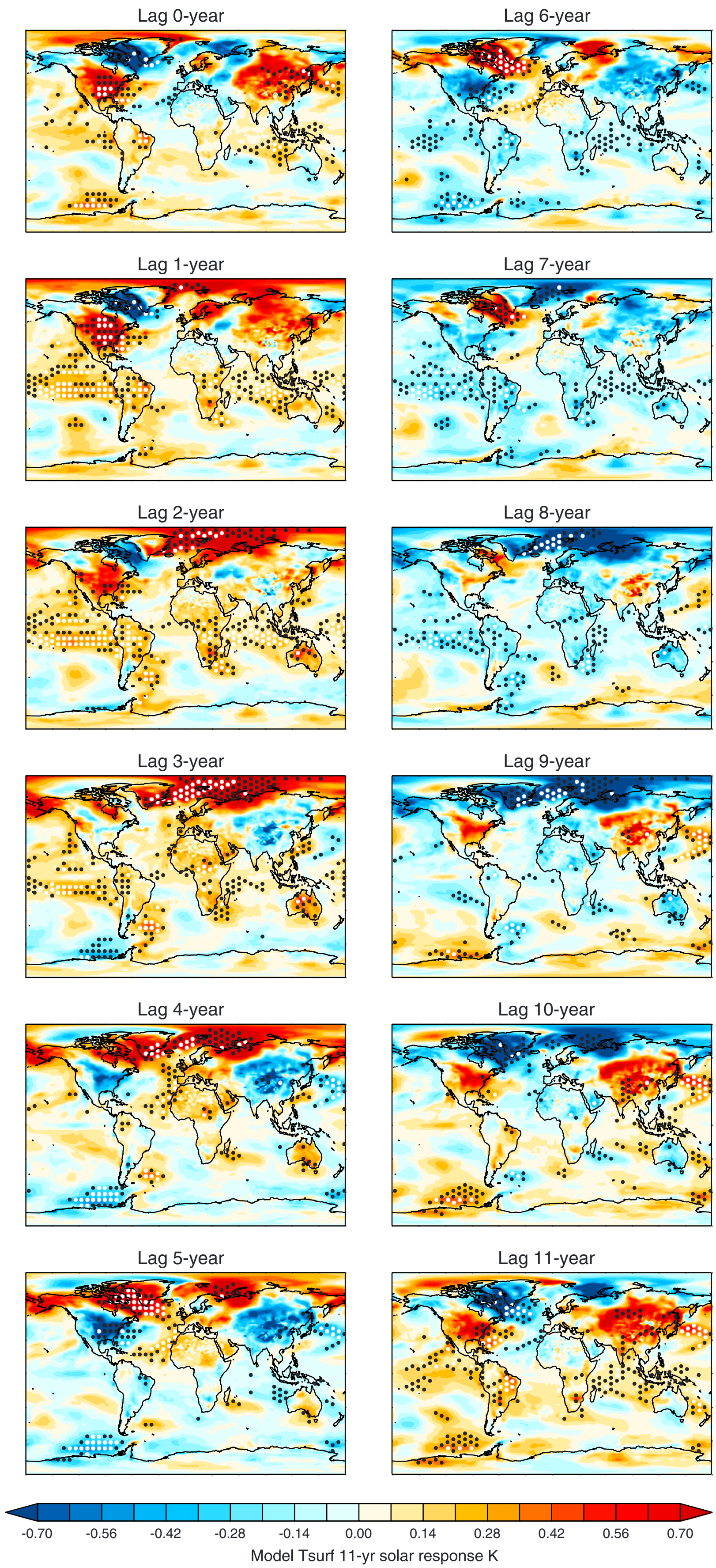

Figure 9. As Figure 5 but from the climate model simulations.

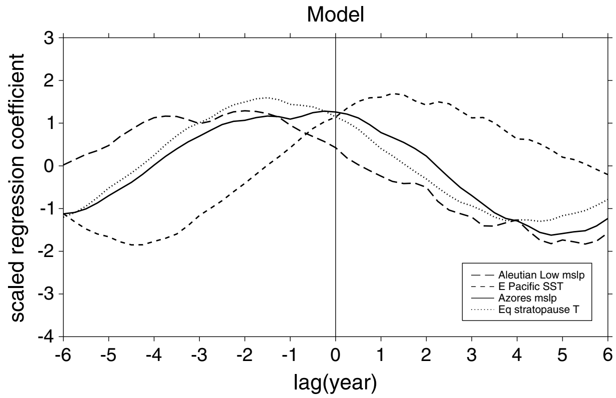

Figure 10. As Figure 6 but from the climate model simulations.

the region of the Azores similar to that seen in the observations, but the maximum anomaly coincides with the solar maximum (zero lag) instead of at the observed 3–4 year lag after solar maximum. A positive anomaly in the Aleutian Low region is present around lag zero, but it is much weaker and has less statistical significance. The surface temperature response (Figure 9) shows the typical quadrupole temperature distribution at lag zero in response to a positive NAO signal, with significant cooling/warming over the Labrador Sea/North America region and corresponding (but not statistically significant) warming/cooling over northern/southern Europe. The Labrador Sea anomaly and the extension of the North American anomaly across the Atlantic, e.g., at zero lag, are similar to the lower part of the tripolar signal that develops in the observed SST response at 2–4 year lags (see Figure 5). At equatorial regions, in contrast to the observed signal (Figure 5), the model shows a broad region of anomalous warming that maximizes at 1–2 year lags across virtually the entire equatorial region, approximately 2 years earlier than in the observations. We note that this broad region of warming across the Pacific does not show a particular resemblance to the ENSO signal, for example, the warming along the west coast of North America is missing. The model also shows a significant signal in the high Arctic region that maximizes at 2–4 years which is not evident in the observational analysis. Finally, the SW-NE banded structure seen in the North Pacific in the observational analysis is absent.

[47] In order to better compare the time evolution of the simulated solar signal with the observations in Figure 6, Figure 10 shows the time evolution of the corresponding modeled regional solar anomalies in mslp over the Azores and Aleutian Low region, the SST anomaly in the East Pacific and the equatorial stratopause temperature anomaly. Comparison with the observations in Figure 6 shows some interesting differences. The stratospheric response maximizes at around 1–2 years before solar maximum, slightly earlier than in the observations. As already noted, the model captures the solar mslp response in the Azores region except that the response is much too rapid when compared with observations, peaking at lag zero instead of at lags of 3–4 years. Similarly, the Aleutian mslp response is rather earlier in the model than in the observations, with a maximum response 2–4 years before solar maximum instead of around zero lag, and precedes the stratospheric response instead of following it. The East Pacific SST response is also too rapid in the model, with a peak response approximately one year after solar max instead of 3–4 years after solar maximum.

[48] Previous climate model experiments have had mixed results in terms of their representation of the 11 year solar response at the Earth's surface. For example, *Meehl et al.* [2009] examined the Pacific response in the Whole Atmosphere Community Climate Model (WACCM) and simulated a La Niña-like SST response to solar maximum conditions (i.e., opposite to the signal in Figure 9) but do not show the North Atlantic region nor the mslp response in either region. *Bal et al*. [2011] using the relatively coarse EGMAM model (ECHO-G with Middle Atmosphere Model; T30 horizontal; 39 levels to 80 km) reproduced the observed mslp anomaly in the vicinity of the Aleutian Low and also found a La Niña-like anomaly in the tropical Pacific but did not examine the Atlantic/European sector. *Petrick et al.* [2012] analyzed the solar signal in the WACCM model with and without a QBO; their main signal in mslp was over the Southern Ocean, but nothing of statistical significance was simulated elsewhere (and they do not show SST responses). *Misios and Schmidt* [2012] examined the SST response (but not the mslp response) in the MAECHAM5 (Middle Atmosphere version of the ECHAM5 model) model and found, in contrast to the WACCM and EGMAM models, a broad warming over equatorial regions in phase with the 11 year solar cycle, similar to that seen in the HadGEM model (Figure 8), but they did not examine the lagged response. Thus, there is little consensus among the model simulations.

5. Summary and Discussion

[49] Observational data for the period 1870–2010 have been analyzed using a lagged multilinear regression technique to isolate the spatial and temporal characteristics of the 11 year solar cycle signals in mslp and SSTs. At zero lag, the mslp analysis confirms the positive anomaly during solar maximum previously identified in the region of the Aleutian Low. In the Atlantic/European sector, there is a weak negative response in the Icelandic region, similar to that found by *Brugnara et al.* [2013], but the signal is not statistically significant. A weak response in the equatorial Pacific sea surface temperatures was identified, similar to the results of *van Loon et al*. [2007], but it is not identical to the ENSO response pattern. In the North Pacific, SST anomalies were identified that resemble the signature of the Pacific Decadal Oscillation.

[50] When the regression analysis was repeated with the surface observations *lagging* the solar index, an additional major feature was identified in the North Atlantic/European sector. The lagged signal (see Figure 4) resembles a positive NAO response and maximizes approximately 3–4 years after the solar maximum. The signal over the Azores region is statistically significant at the 99% level. The corresponding SST anomalies in the North Atlantic (Figure 5) are consistent with this, both spatially and temporally. Although evidence for a lagged response was noted in a previous study by *Qun and Quiming* [1993], their result has largely gone unnoticed. A similar lagged response is identified in the recent study by *Hood et al*. [2013], although they concentrated on the Pacific response and only extended their analysis to lags of up to 2 years.

[51] Having identified a lagged NAO-like response in observations over the Atlantic/European sector, the challenge

is to identify a possible mechanism. As noted in section 3, a prime mechanism for a surface solar influence at high latitudes is via the stratosphere, but Figure 6 shows that the observed stratospheric temperature anomaly maximizes at approximately zero lag or slightly before. While there may be a small time delay for this anomaly to transfer from the stratosphere down to the surface, this is unlikely to be more than a year, so cannot explain a 3–4 year lagged response.

[52] One possibility is that the index employed may not be the optimum index to represent solar variability. To check this, results of the multilinear regression analysis of the observations using different solar indices were compared. Using sunspot number and TSI, *Lean* [2009] gave nearly identical results, with a 3–4 year lagged response at the surface in the Atlantic/European sector. Open solar flux (OSF) peaks slightly later than the TSI and has been proposed as an alternative index that better characterizes UV variability [*Woollings et al*., 2010]. Repeating the analysis with OSF as the solar index gives a maximum mslp response at 2–3 year instead of 3–4 year lags, so this can account for a 1 year lag at most.

[53] *Scaife et al*. [2013] proposed that a feedback between the atmosphere and ocean might explain the lagged response in the North Atlantic/European region. Almost 50 years ago, *Bjerknes* [1964] demonstrated that interannual variability in Atlantic SSTs is primarily a response to atmospheric forcing through wind stress and heat fluxes, but he also conjectured that the SST variations would in turn feed back onto the atmosphere. The latter has since been confirmed by observational studies [*Rodwell and Folland*, 2002; *Taws et al*., 2011]. Thermal anomalies created in the ocean mixed-layer by atmospheric forcing in winter were found to be submerged and preserved below the shallow summer mixed layer, subsequently reemerging in the following autumn, thus serving to reinforce and perpetuate the original NAO anomaly into the next winter. In addition, multimodel ensemble studies of coupled atmosphere-ocean climate simulations have highlighted the influence of multidecadal stratospheric variability on the North Atlantic Ocean [e.g., *Eden and Jung*, 2001; *Keenlyside et al*., 2008; *Reichler et al*., 2012; *Greatbach et al*., 2012], and model studies specifically investigating stratosphere-ocean feedbacks [*Yukimoto and Kodera*, 2007] found that the oceanic response had a positive feedback effect on the NAO, implying enforcement/maintenance of the surface response to the stratospheric forcing. All of these studies support a mechanism whereby a relatively weak NAO anomaly forced in consecutive years by a stratospheric circulation anomaly could be amplified and perpetuated through local ocean-atmosphere feedback processes. Examination of the timing of the signals in Figures 3 and 4 supports this mechanism, since the SST response (Figure 4) peaks slightly earlier at 2–3 year lags than the mean sea level response (Figure 4) which peaks at 3–4 year lags.

[54] This hypothesis was tested by *Scaife et al*. [2013] by looking at the transient response to solar forcing using a version of the same HadGEM coupled atmosphere-ocean climate model [see also *Ineson et al*., 2011]. They found that the response to a step change in solar forcing has an immediate atmospheric signature (that projected onto the NAO) but accumulated in the ocean over several years, during which time the atmospheric response also increased, similar to that seen in Figure 3. They proposed a coupled positive feedback between the atmosphere and Atlantic Ocean in which the Atlantic Ocean provides the means by which the solar anomaly is able to persist. They found plausible parameters for the coupled interactions of the different components, i.e., the strength and persistence of the various feedbacks, but noted that stronger atmosphere-ocean coupling than implied by the climate model is required to reproduce the lagged response seen in the observations.

[55] This suggestion of insufficiently strong coupling between atmosphere and ocean in the climate model is further supported by the modeling results presented in section 4, in which the 11 year solar signal was examined in very long simulations of the HadGEM ocean-atmosphere coupled climate model. The upper boundary of the model is at 84 km, so that the (top-down) mechanism for solar influence via UV irradiance influence on the stratosphere is included in the model, in addition to the more standard (bottom-up) mechanism via changes in the visible part of the spectrum that penetrate directly to the surface. The model simulation of the solar response in the stratosphere compares reasonably well with observational analyses, with equatorial stratopause temperatures rapidly responding to the solar cycle variations, although it is not clear why the response occurs (in both the model and the observations) slightly before the solar maximum. One possibility is that there is a feedback between the solar response in equatorial SSTs that then generates anomalous tropospheric wave forcing from the troposphere into the stratosphere.

[56] The model also reproduces the spatial pattern of the surface response in the North Atlantic/European sector, with a positive NAO-like response in solar maximum years and a corresponding surface temperature quadrupole response that is consistent with this. However, the modeled mslp field responded almost immediately to the solar variations so that the maximum response coincided with solar maximum, instead of the observed 3–4 year lagged response (Figure 10). This suggests that if the mechanism proposed by *Scaife et al*. [2013] is responsible for the lagged response, then the coupling between the atmosphere and Atlantic Ocean in the HadGEM model is far too weak.

[57] In addition, the study shows that the model reproduces the mslp response over the Aleutian region and an SST response in the equatorial Pacific, but the timing of these solar-induced anomalies did not agree well with observations, suggesting a possible problem with the relative influences of the various mechanisms and/or teleconnections that influence the anomalies in these different regions. We also note that there are other mechanisms and interactions that are not well represented in the model. For example, the model has a self-generated QBO, but investigation shows that there is very little interaction between the modeled QBO and solar cycle signals in the polar winter stratosphere. Additionally, there is no representation in the model of alternative mechanisms, e.g., involving geomagnetic variability [*Seppala et al*., 2009].

[58] If the apparent lagged influence of 11 year solar variability on the Atlantic/European sector suggested by the observational analysis is real, it has implications for seasonal to decadal predictability in Europe. There have been some suggestions that the recent solar minimum in 2009 may have contributed to the cold European winters of 2009 and 2010 [*Lockwood et al*., 2010], so improved representation of solar

variability in seasonal weather forecasting models may help to improve their predictive skills. However, there are still many uncertainties, not only in the characterization of the observational signal but also in our understanding of the mechanisms for solar influence. There is currently no consensus between climate models, and this clearly needs to be resolved before implementation in weather prediction models is likely. In addition, there may also be implications for predicting future climate change. If the Sun descends from its current "Grand Maximum" phase toward lower output levels and variability [*Jones et al*., 2012; *Meehl et al*., 2013], then regional impacts of solar variability could potentially mask some of the predicted changes associated with increased levels of greenhouse gases.

[59] **Acknowledgments.** LJG, SO, and RS were supported by the UK Natural Environment Research Council (NERC) National Centre for Atmospheric Science (NCAS). DMM was supported by a NERC response-mode grant. AAS, SI, SH, NB, and JK were supported by the Joint DECC/DEFRA Met Office Hadley Centre Climate Programme (GA01101).

References

Allan, R. J., and T. J. Ansell (2006), A new globally complete monthly historical gridded mean sea level pressure data set (HadSLP2): 1850–2004, *J. Clim.*, *19*, 5816–5842, doi:10.1175/JCLI3937.1.
Bal, S., S. Schimanke, T. Spangehl, and U. Cubasch (2011), On the robustness of the solar cycle signal in the Pacific region, *Geophys. Res. Letts.*, *38*, L14809, doi:10.1029/2011GL047964.
Baldwin, M. P., and T. J. Dunkerton (2001), Stratospheric harbingers of anomalous weather regimes, *Science*, *294*, 581–584, doi:10.1126/science.1063315.
Barriopedro, D., R. Garcia-Herrera, and R. Huth (2008), Solar modulation of Northern Hemisphere winter blocking, *J. Geophys. Res.*, *113*, D14118, doi:10.1029/2008JD009789.
Bjerknes, J. (1964), Atlantic air-sea interactions, *Adv. Geophys.*, *10*, 1–82.
Brugnara, Y., S. Bronnimann, J. Luterbacher, and E. Rozanov (2013), Influence of the sunspot cycle on the Northern Hemisphere wintertime circulation from long upper-air data sets, *Atmos. Chem. Phys.*, *13*, 6275–6288, doi:10.5194/acp-13-6275-2013.
Christoforou, P., and S. Hameed (1997), Solar cycle and the Pacific "centers of action", *Geophys. Res. Letts.*, *24*, 293–296, doi:10.1029/97GL00017.
Cionni, I., V. Eyring, J. F. Lamarque, W. J. Randel, D. S. Steveson, F. Wu, G. E. Bodeker, T. G. Shepherd, D. T. Shindell, and D. W. Waugh (2011), Ozone database in support of CMIP5 simulations: Results and corresponding radiative forcing, *Atmos. Chem. Phys. Discuss.*, *11*, 10,875–10,933, doi:10.5194/acpd-11-10875-2011.
Crooks, S. A., and L. J. Gray (2005), Characterization of the 11-year solar signal using a multiple regression analysis of the ERA-40 data set, *J. Clim.*, *18*, 996–1015, doi:10.1175/JCLI-3308.1.
Deser, C., M. A. Alexander, S.-P. Xie, and A. S. Phillips (2010), Sea surface temperature variability: Patterns and mechanisms, *Annu. Rev. Mar. Sci.*, *2*, 115–143, doi:10.1146/annurev-marine-120408-151453.
Driscoll, S., A. Bozzo, L. J. Gray, A. Robock, and G. Stenchikov (2012), Coupled Model Intercomparison Project (CMIP5) simulations of climate following volcanic eruptions, *J. Geophys. Res.*, *117*, D17105, doi:10.1029/2012JD017607.
Eden, C., and T. Jung (2001), North Atlantic interdecadal variability: Oceanic response to the North Atlantic Oscillation (1865–1997), *J. Clim.*, *14*, 676–691.
Ermolli, I., et al. (2013), Recent variability of the solar spectral irradiance and its impact on climate modelling, *Atmos. Chem. Phys.*, *13*, 3945–3977, doi:10.5194/acp-13-3945-2013.
Frame, T. H. A., and L. J. Gray (2010), The 11-year solar cycle in ERA-40 data: An update to 2008, *J. Clim.*, *23*, 2213–2222, doi:10.1175/2009JCLI3150.1.
Gray, L. J., S. T. Rumbold, and K. P. Shine (2009), Stratospheric temperature and radiative forcing response to 11-year solar cycle changes in irradiance and ozone, *J. Atmos. Sci.*, *66*, 2402–2417, doi:10.1175/2009JAS2866.1.
Gray, L. J. J., et al. (2010), Solar influences on climate, *Rev. Geophys.*, *48*, RG4001, doi:10.1029/2009RG000282.
Greatbach, R. J., G. Gollan, T. Jung, and T. Kunz (2012), Factors influencing Northern Hemisphere winter mean atmospheric circulation anomalies during the period 1960/61 to 2001/02, *Q. J. R. Meteorol. Soc.*, *138*, 1970–1982.
Haam, E., and K. K. Tung (2012), Statistics of solar cycle—La Niña connection: Correlation of two autocorrelated time series, *J. Atmos. Sci.*, *69*, 2934–2939.
Haigh, J. D. (1996), The impact of solar variability on climate, *Science*, *272*, 981–984, doi:10.1126/science.272.5264.981.
Haigh, J. D. (2003), The effects of solar variability on the Earth's climate, *Philos. Trans. R. Soc. London Ser. A*, *361*, 95–111, doi:10.1098/rsta.2002.1111.
Haigh, J. D., and M. Blackburn (2006), Solar influences on dynamical coupling between the stratosphere and troposphere, *Space Sci. Rev.*, *125*, 331–344, doi:10.1007/s11214-006-9067-0.
Hardiman, S. C., N. Butchart, S. M. Osprey, L. J. Gray, A. C. Bushell, and T. J. Hinton (2010), The climatology of the middle atmosphere in a vertically extended version of the Met Office's climate model. Part I: Mean state, *J. Atmos. Sci.*, *67*(5), 1509–1525, doi:10.1175/2009JAS3337.1.
Hardiman, S. C., N. Butchart, T. J. Hinton, S. M. Osprey, and L. J. Gray (2012), The effect of a well-resolved stratosphere on surface climate: Differences between CMIP5 simulations with high and low top versions of the Met Office Climate Model, *J. Clim.*, *25*, 7083–7099, doi:10.1175/JCLI-D-11-00579.1.
Hood, L., S. Schimanke, T. Spangehl, S. Bal, and U. Cubasch (2013), The surface climate responses to 11-yr solar forcing during northern winter: Observational analyses and comparisons with GCM simulations, *J. Clim.*, doi:10.1175/JCLI-D-12-00843.1.
Ineson, S., A. A. Scaife, J. R. Knight, J. C. Manners, N. J. Dunstone, L. J. Gray, and J. D. Haigh (2011), Solar forcing of winter climate variability in the northern hemisphere, *Nat. Geosci.*, *4*, doi:10.1038/NGEO1282.
Ingram, W. J. (2006), Detection and attribution of climate change and understanding solar influence on climate, *Space Sci. Rev.*, *125*, 199–211.
Intergovernmental Panel on Climate Change (2007), *Climate Change 2007: The Physical Science Basis—Contribution of Working Group I to the Fourth Assessment Report of the Inter-Governmental Panel on Climate Change*, edited by S. Solomon et al., Cambridge Univ. Press, Cambridge, U. K.
Jones, P. D., T. Jonsson, and D. Wheeler (1997), Extension to the North Atlantic Oscillation using early instrumental pressure observations from Gibraltar and south-west Iceland, *Int. J. Clim.*, *17*, 1433–1450.
Jones, C. D., et al. (2011), The HadGEM2-ES implementation of CMIP5 centennial simulations, *Geosci. Model Dev.*, *4*, 543–570, doi:10.5194/gmd-4-543-2011.
Jones, G. S., M. Lockwood, and P. A. Stott (2012), What influence will future solar activity changes over the 21st century have on projected global near-surface temperature changes?, *J. Geophys. Res.*, *117*, D05103, doi:10.1029/2011JD017013.
Keenlyside, N. S., M. Latif, J. Jungclaus, L. Kornblueh, and E. Roeckner (2008), Advancing decadal-scale climate prediction in the North Atlantic sector, *Nature*, *453*, 84–88.
Kodera, K. (1995), On the origin and nature of the interannual variability of the winter stratosphere circulation in the northern hemisphere, *J. Geophys. Res.*, *100*, 14,077–14,087.
Kodera, K. (2002), Solar modulation of the North Atlantic Oscillation: Implications in the spatial structure of the NAO, *Geophys. Res. Letts.*, *29*(8), 1218, doi:10.1029/2001GL014557.
Kodera, K. (2003), Solar influence on the spatial structure of the NAO during the winter 1900–1999, *Geophys. Res. Letts.*, *30*, doi:10.1029/2002GL016584.
Kodera, K., and Y. Kuroda (2002), Dynamical response to the solar cycle: Winter stratopause and lower stratosphere, *J. Geophys. Res.*, *107*(D24), 4749, doi:10.1029/2002JD002224.
Kuroda, Y., and K. Kodera (2004), Role of the Polar-night Jet Oscillation on the formation of the Arctic Oscillation in the Northern Hemisphere winter, *J. Geophys. Res.*, *109*, D11112, doi:10.1029/2003JD004123.
Labitzke, K. (1987), Sunspots, the QBO and the stratospheric temperature in the north polar region, *Geophys. Res. Lett.*, *14*, 535–537.
Labitzke, K., M. Kunze, and S. Bronnimann (2006), Sunspots, the QBO and the stratosphere in the north polar region—20 years later, *Meterol. Z.*, *15*, 355–363, doi:10.1127/0941-2948/2006/0136.
Lean, J. L. (2009), Available at http://www.geo.fu-berlin.de/en/met/ag/strat/forschung/SOLARIS/Input_data/Calculations.of.Solar.Irradiance.pdf last access: 2 June 2009.
Lean, J. L., and D. H. Rind (2008), How natural and anthropogenic influences alter global and regional surface temperatures: 1889 to 2006, *Geophys. Res. Letts.*, *35*, L18701, doi:10.1029/2008GL034864.
Lean, J. L., and D. H. Rind (2009), How will Earth's surface temperature change in future decades?, *Geophys. Res. Letts.*, *36*, L15708, doi:10.1029/2009GL038932.
Lockwood, M., R. G. Harrison, T. J. Woollings, and S. Solanki (2010), Are cold winters in Europe associated with low solar activity?, *Environ. Res. Lett.*, *5*, 024001, doi:10.1088/1748-9326/5/2/024001.
Lorenz, E. N. (1963), Deterministic nonperiodic flow, *J. Atmos. Sci.*, *20*, 130–141.
Luterbacher, J., E. Xoplaki, D. Dietrich, R. Rickli, J. Jacobeit, C. Beck, D. Gyalistras, C. Schmutz, and H. Wanner (2002), Reconstruction of sea

level pressure fields over the eastern North Atlantic and Europe back to 1500, *Clim. Dyn.*, *18*, 545–561, doi:10.1007/S00382-001-0196-6.

Mann, M. E., Z. Zhang, S. Rutherford, R. S. Bradley, M. K. Hughes, D. Shindell, C. Ammann, G. Faluvegi, and F. Ni (2009), Global signatures of the little ice age and medieval climate anomaly and plausible dynamical origins, *Science*, *326*, 1256–1260.

Martin, G. M., et al. (2011), The HadGEM2 family of Met Office Unified Model climate configurations, *Geosci Model Dev*, *4*(3), 723–757, doi:10.5194/gmd-4-723-2011.

Matthes, K., U. Langematz, L. J. Gray, K. Kodera, and K. Labitzke (2004), Improved 11-year solar signal in the Freie Universitat Berlin Climate Middle Atmosphere Model (FUB-CMAM), *J. Geophys. Res.*, *109*, D06101, doi:10.1029/2003JD004012.

Matthes, K., Y. Kuroda, K. Kodera, and U. Langematz (2006), Transfer of the solar signal from the stratosphere to the troposphere: Northern winter, *J. Geophys. Res.*, *111*, D06108, doi:10.1029/2005JD006283.

Meehl, G. A., and J. M. Arblaster (2009), A lagged warm event-like response to peaks in solar forcing in the Pacific region, *J. Clim.*, *22*(13), 3647–3660.

Meehl, G. A., J. M. Arblaster, G. Branstator, and H. van Loon (2008), A coupled air-sea response mechanism to solar forcing in the Pacific region, *J. Clim.*, *21*, 2883–2897, doi:10.1175/2007JCLI776.1.

Meehl, G. A., J. M. Arblaster, K. Matthes, F. Sassi, and H. van Loon (2009), Amplifying the Pacific climate system response to a small 11-year solar cycle forcing, *Science*, *325*, 1114–1118, doi:10.1126/science.1172872.

Meehl, G. A., J. M. Arblaster, and D. R. Marsh (2013), Could a future "Grand Solar Minimum" like the Maunder Minimum stop global warming?, *Geophys. Res. Letts.*, *40*, 1789–1793, doi:10.1002/grl.50361.

Misios, S., and H. Schmidt (2012), Mechanisms involved in the amplification of the 11-yr solar cycle signal in the tropical Pacific Ocean, *J. Clim.*, *25*, 5102–5118, doi:10.1175/JCLI-D-11-00261.1.

Mitchell, D. M., L. J. Gray, J. Anstey, M. P. Baldwin, and A. J. Charlton-Perez (2013), The influence of stratospheric vortex displacements and splits on surface climate, *J. Clim.*, *26*(8), 2668–2682.

Osprey, S. M., L. J. Gray, S. C. Hardiman, N. Butchart, A. C. Bushell, and T. J. Hinton (2010), The climatology of the middle atmosphere in a vertically extended version of the Met Office's climate model. Part II: Variability, *J. Atmos. Sci.*, *67*(11), 3637–3651, doi:10.1175/2010JAS2228.1.

Petrick, C., K. Matthes, H. Dobslaw, and M. Thomas (2012), Impact of the solar cycle and the QBO on the atmosphere and the ocean, *J. Geophys. Res.*, *117*, D17111, doi:10.1029/2011JD017390.

Pittock, A. B. (1978), A critical look at long-term sun-weather relationships, *Rev. Geophys.*, *16*, 400–420.

Pittock, A. B. (1983), Solar variability, weather and climate: An update, *Q. J. R. Meteorol. Soc.*, *109*, 23–55.

Pittock, A. B. (2009), Can solar variations explain variations in the Earth's climate?, *Clim. Change*, *96*, 483–487.

Qun, X., and Y. Quiming (1993), Response of the intensity of the subtropical high in the northern hemisphere to solar activity, *Adv. Atmos. Sci.*, *10*, 325–334.

Randel, W. J., and F. Wu (1999), A stratospheric ozone trends data set for global modeling studies, *Geophys. Res. Lett.*, *26*, 3089–3092.

Rayner, N. A., et al. (2003), Global analyses of sea surface temperature, sea ice, and night marine air temperature since the late nineteenth century, *J. Geophys. Res.*, *108*(D14), 4407, doi:10.1029/2002JD002670.

Reichler, T., J. Kim, E. Manzini, and J. Kroger (2012), A stratospheric connection to Atlantic climate variability, *Nat. Geosci.*, *5*, 783–787, doi:10.1038/NGEO1586.

Rodwell, M. J. (2003), On the predictability of North Atlantic climate, in *The North Atlantic Oscillation, Climatic Significance and Environmental Impact*, Geophys. Monogr., vol. 134, edited by J. W. Hurrell et al., pp. 173–192, AGU, Washington, D. C.

Rodwell, M. J., and C. K. Folland (2002), Atlantic air-sea interaction and seasonal predictability, *Q. J. R. Meteorol. Soc.*, *128*, 1413–1443.

Roy, I., and J. D. Haigh (2010), Solar cycle signals in sea level pressure and sea surface temperature, *Atmos. Chem. Phys.*, *10*, 3147–3153.

Roy, I., and J. Haigh (2012), Solar cycle signals in the Pacific and the issue of timings, *J. Atmos. Sci.*, *69*, 1446–1451, doi:10.1175/JAS-D-11-0277.1.

Sato, M., J. Hansen, M. McCormick, and J. Pollack (1993), Stratospheric aerosol optical depths, *J. Geophys. Res.*, *98*, 22,987–22,994, doi:10.1029/93JD02553.

Scaife, A. A., N. Butchart, C. D. Warner, and R. Swinbank (2002), Impact of a spectral gravity wave parametrization on the stratosphere in the Met Office Unified Model, *J. Atmos. Sci.*, *59*, 1473–1489.

Scaife, A. A., S. Ineson, J. R. Knight, L. J. Gray, K. Kodera, and D. M. Smith (2013), A mechanism for lagged North Atlantic climate response to solar variability, *Geophys. Res. Letts.*, *40*, 434–439, doi:10.1002/grl.50099.

Schneider, N., and B. D. Cornuelle (2005), The forcing of the Pacific Decadal Oscillation, *J. Clim.*, *18*, 4355–4373, doi:10.1175/JCLI3527.1.

Seppala, A., C. E. Randall, M. A. Clilverd, E. Rozanov, and C. J. Rodgers (2009), Geomagnetic activity and polar surface air temperature variability, *J. Geophys. Res.*, *114*, A10312, doi:10.1029/2008JA014029.

Stott, P. A., G. S. Jones, J. A. Lowe, P. Thorne, S. Durham, T. C. Johns, and J.-C. Thelen (2006), Transient climate simulations with the HadGEM1 climate model: Causes of past warming and future climate change, *J. Clim.*, *19*, 2763–2782.

Taws, S. L., R. Marsh, N. C. Wells, and J. Hirschi (2011), Re-emerging ocean temperature anomalies in late-2010 associated with a repeat negative NAO, *Geophys. Res. Letts.*, *38*, L20601, doi:10.1029/2011GL048978.

van Loon, H., and G. Meehl (2008), The response in the Pacific to the sun's decadal peaks and contrasts to cold events in the Southern Oscillation, *J. Atmos. Sol. Terr. Phys.*, *70*, 1046–1055.

van Loon, H., G. A. Meehl, and D. Shea (2007), The effect of the decadal solar oscillation in the Pacific troposphere in northern winter, *J. Geophys. Res.*, *112*, D02108, doi:10.1029/2006JD007378.

Van Oldenborgh, G. J., A. T. J. de Laat, J. Luterbacher, W. J. Ingram, and T. J. Osborn (2013), Claim of solar influence is on thin ice: Are 11-yearcycle solar minima associated with severe winters in Europe?, *Environ. Res. Lett.*, *8*, 024014, doi:10.1088/1748-9326/8/2/024014.

Visbeck, M. H., J. W. Hurrell, L. Polvanis, and H. M. Cullen (2001), The North Atlantic Oscillation: Past, present, and future, *Proc. Natl. Acad. Sci. U.S.A.*, *98*, 12,876–12,877.

Wang, Y.-M., L. J. Lean, and N. R. Sheeley Jr. (2005), Modeling the Sun's magnetic field and irradiance since 1713, *Astrophys. J.*, *625*, 522–538.

Warner, C. D., and M. E. McIntyre (1999), Toward an ultra-simple spectral gravity wave parametrization for general circulation models, *Earth Planets Space*, *51*, Terra Scientific, 475–484.

Woollings T., M. Lockwood, G. Masato, C. Bell, and L. J. Gray (2010), Enhanced signature of solar variability in Eurasian winter climate, *Geophys. Res. Letts.*, *37*, L20805, doi:10.1029/2010GL044601.

Yukimoto, S., and K. Kodera (2007), Annular modes forced from the stratosphere and interactions with the ocean, *J. Meteorol. Soc. Jpn.*, *85*, 943–952.

Zhou, J., and K. K. Tung (2010), Solar cycles in 150 years of global sea surface temperature data, *J. Clim.*, doi:10.1175/2010JCL13232.1.

Zhou, J., and K. K. Tung (2013), Observed tropospheric temperature response to 11-yr solar cycle and what it reveals about mechanisms, *J. Atmos. Sci.*, *70*, 9–14, doi:10.1175/JAS-D-12-0214.1.